

Is Guanine(G) Tautomer Interaction Responsible For The Existence Of GG Mismatches? A Quantum Mechanical Studies On G Tautomer Combination?

J. Basumatary

B. Bezbaruah

¹Department of Applied Sciences, GUIST, Guwahati

T. K. Barman

C. Medhi

Department, Gauhati University, P.O,Gauhati University,
Guwahati

Abstract: Density functional theory and MP2 level of studies on the pairing of G tautomers are performed to understand the existence of GG mismatches in DNA. Some metastable GG pairs are found favorable, which in fact may be relevant for explaining the GG mismatches in DNA. Several types of H-bonds are found in these metastable GG combinations. The H bonds (a) $>N...H-N<$ (between ring N) (b) $-O-H...O=C-$ (keto-enol) types are found to be very important in these stable structures. The structure and stability of GG pairing from G tautomers depend on the types of H bonds present in these pairs. The most stable metastable GG combination is G2-cisG4, whereas the H bond characteristic in transG4-1cisG5 combination is quite close to available crystal structure.

Keywords: Mismatches, GG pairing, H-bond, Metastable, B3LYP, MP2, Tautomers.

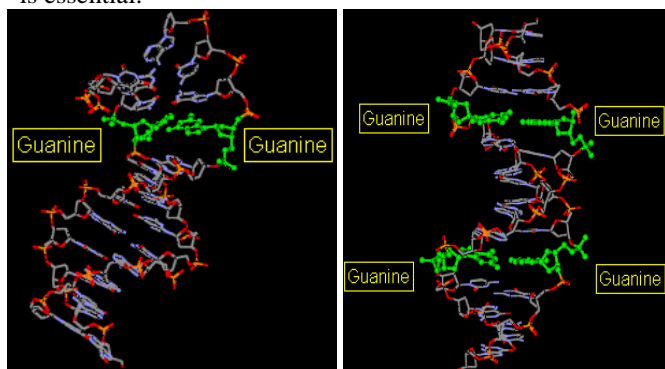
I. INTRODUCTION

There are several of non-complementary GG pairings in duplex DNA. The presence of these GG mismatches may usually lead to destabilization of DNA helical structure, which may be due to conformational change at the GG pairing region (Figures 1.1(i-ii)) [1-11]. Although two important interactions such as hydrogen bonding and stacking of aromatic rings contribute to the stabilization of a helical conformation, several other factors may be involved for the destabilization of helical structure [4, 12-14]. Some GG mismatches are detected in the crystal structures of DNA [5-7]. It has been observed that the hydrogen bonds between G and G in these GG mismatches are somewhat distorted or twisted and also somewhat stacked with the adjacent nucleobases (Figures 1(i-ii)). The contributions of these two types of interactions to the stability of GG pairs are rather important. These GG mismatches may appear during mutagenic pathway which is likely to be corrected subsequently. Therefore, the origin of metastable GG mismatches shown in Figures 1(i-ii) and 2(i-ii) may be analysed with respect to different types of H bonds.

The information may be useful to understand the repair mechanism of these types of mismatches. The structures of available non-complementary GG mismatches are not exactly similar. In fact the tautomeric forms of G may be involved in the formation of GG mismatches on subsequent destabilization of WC GC [7-10]. Some tautomers of G are shown in Figure 3. The less stable tautomers are likely to interact forming several GG mismatches (Figure 4). However, there may be various ways of generating GG mismatches, but the effects of proton, water molecules and metal ion are considered as important factors [12-20]. So there are fair possibilities of forming metastable GG mismatches on subsequent tautomerization of G tautomers. Several metastable GG mismatches shown in Figure 4 have been taken up in this investigation. The geometries of these base pairs are constructed with respect to symmetric syn-syn, anti-syn, syn-anti conformers of tautomer G for pairing with another G through H bonds (Figure 4). Hydrogen bonding is considered as the main interaction responsible for metastable GG pairing.

The importance of quantum mechanical calculations in dealing this type of problem has been highlighted in several

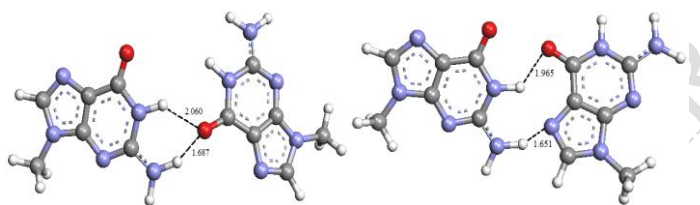
contexts. One of the successes of *ab initio* calculation is the accurate estimation of hydrogen bonding capacity of molecules. Similarly, the methods may be used for understanding of the formation of GG pairs [15-25]. It has been already explained in many contexts that such mispairing may sometimes lead to chronic diseases like cancer, but how these mispairs occur instead of stable WC pairs has not been explored. It is essential to investigate hydrogen bonding capacity in metastable GG combination for explaining the experimentally found GG mismatches in certain sequences of DNA (Figures 1(i-ii) and 2(i-ii)). Hence, understanding of metastable GG mismatches formed through suitable H-bonds is essential.



(i) 1OH7

(ii) 1D80

Figures 1(i-ii): (i) Crystal structure from pdb 1OH7 and (ii) Crystal structure from pdb 1D80



(i) 1OH7

(ii) 1D80

Figures 2(i-ii): GG pairing obtained from crystal structures (pdb) (i) 1OH7, and (ii) 1D80. All the hydrogen bond lengths in above figures are in angstrom unit (Å)

II. METHODOLOGY

Initially, the geometries of G tautomers were completely optimized with quantum mechanical methods using Gaussian 03 program code [26]. We have used B3LYP with basis sets 6-31+G(d,p) and 6-31++G(d,p) for optimizing the geometries of G tautomers and metastable GG pairs (Figures 3 and 4). For such hydrogen bonded system it is essential to include electron correlation and BSSE corrections in the calculations [15-25]. Also the basis set 6-31++G(d,p) that include p-type polarization functions on H atoms is essential in dealing with hydrogen bonding systems.

In many studies B3LYP method with 6-31++G(d,p) and even HF with 6-31+G(d,p) method are used successfully for similar type of H-bonded system. In the sense that electronic energies contributed for the stabilization of H-bonded system can also be used for comparing the stability of several GG mismatches. However, we have performed single point MP2/6-31+G(d,p) calculations on the optimized geometries of

B3LYP/6-31+G(d,p) for comparison with results of B3LYP calculations. We have estimated BSSE values to understand the errors in the interaction energies obtained from these two methods, and also other thermodynamic properties are calculated for these metastable GG mismatches. The BSSE values were computed by using counterpoise method adopted in Gaussian 03 program package [26]. The structures and energetic of these metastable GG pairs are analysed. Moreover, the thermodynamics parameters of these GG pairs are used to explain the sensitivity and stability of geometries.

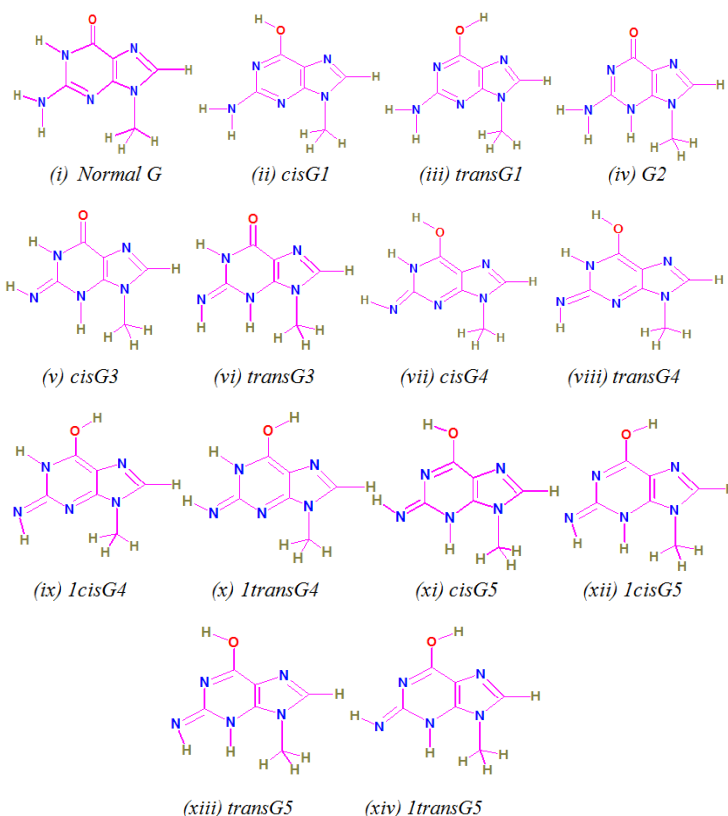
The interaction energies and thermodynamic properties of metastable GG mismatches are computed from the following equations.

ΔE = Electronic energies of GG pair – (sum of Electronic energies of two G tautomers).

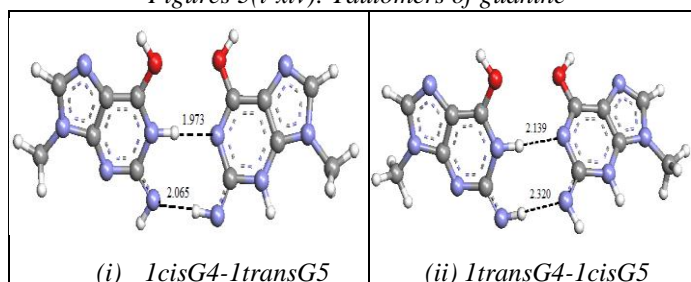
ΔG = Free energy of GG pair – (sum of the Free energies of two G tautomers).

ΔH = Enthalpy of GG pair – (sum of Enthalpies of two G tautomers).

ΔZPE = Zero point energy of GG pair – (sum of Zero point Energy of two G tautomers).

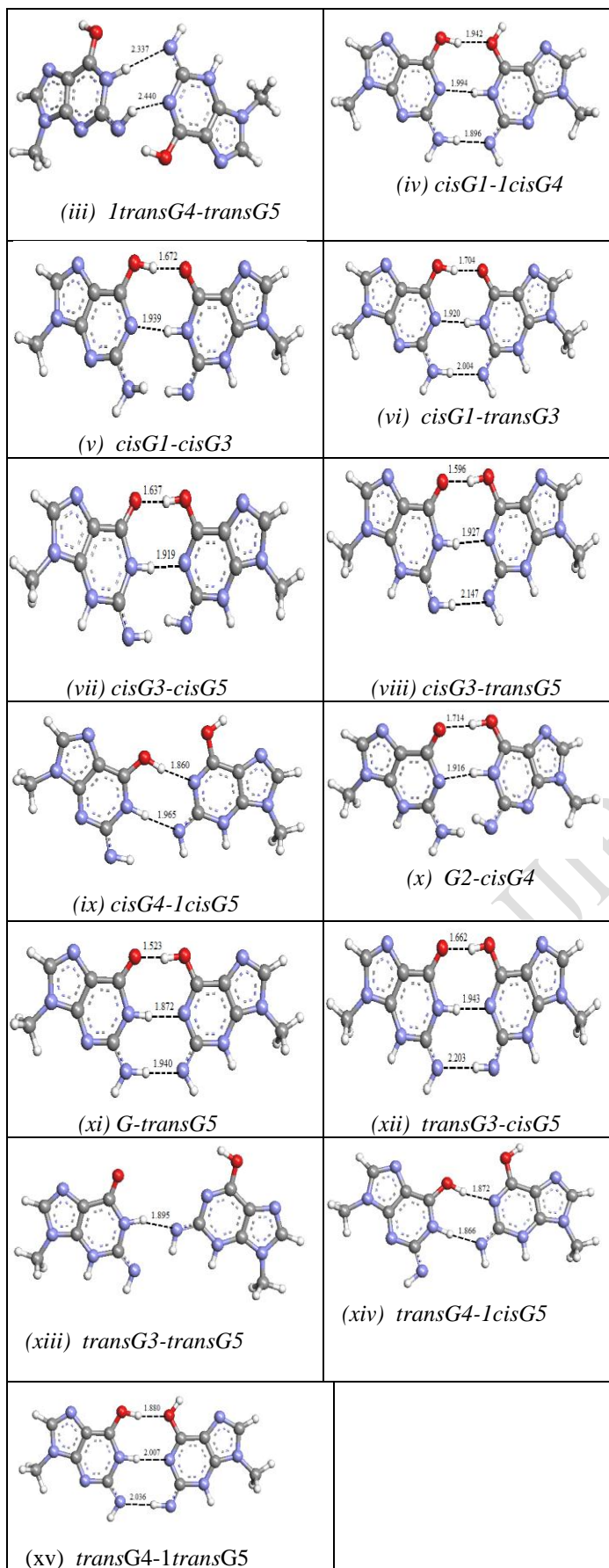


Figures 3(i-xiv): Tautomers of guanine



(i) 1cisG4-1transG5

(ii) 1transG4-1cisG5



Figures 4(i-xv): Structures of metastable GG mismatches (6-31++G(d,p)). (All the hydrogen bond lengths in above figures are in angstrom unit (Å))

III. RESULTS AND DISCUSSION

The interaction energies of metastable GG mismatches computed with B3LYP with basis sets 6-31+G(d,p) and B3LYP/6-31++G(d,p) (Tables 1 and 2). The interaction energies of single point MP2/6-31+G(d,p) calculations on the B3LYP/6-31+G(d,p) optimized geometry are also carried out (Table 3). The interaction energies of all these metastable GG pairs are found significantly different, hence the nature of bonding in these metastable GG pairs may be analysed. The corresponding values obtained from HF/6-31+G(d,p) are also computed for comparison with those of other calculations (Table 4). Moreover, the thermodynamic properties are also computed to predict the stability of these mismatches (Table 5). The formation of metastable GG pairs may be analysed with respect to the H bonding types, which are not distinctly indicated in crystal structures [5-7]. The pattern of H-bonds observed in these metastable GG pairs may be taken up to explain the existence of GG mismatches in DNA. Different types of H-bonds are found in all these metastable GG pairs. The structures and different types of H bonds in GG pairs are shown in Figures 4 and Table 6. The hydrogen bonding capacity of different types of H-bonds may be used for explaining the structures and stability of metastable GG mismatches (Table 6).

This existence of purine-purine mismatches usually leads to transversion mutation in daughter DNA strands during repair mechanism. Hence, recognition of certain sites during the formation of metastable GG mismatches for H-bonding is very important. It also determines what type of mismatches can be formed when two G tautomers come in close contact for pairing. Also the conformational changes in DNA due to the presence of stable GG pairs are observed very significant [17-19]. In most of the investigations the generation of G tautomers as a result of the destabilization of GC base pairs under various conditions has been found. As we know that guanine is very sensitive towards slight change in the physico-chemical properties of surrounding solution. Henceforth, in most GG pairs keto-enol interactions at the syn and anti conformations of individual G are found (Figure 3.4). However, there are several possibilities of forming G tautomer combinations. It is possible to understand the stability of several GG mismatches the H-bonding types in metastable GG pairs. Understanding of such metastable GG pairs is essential to explain how GG mismatches are formed in DNA sequences. The molecular structures of GG mismatches available in crystal structures do not distinctly indicate different types of H-bonds. Assuming that tautomers of G may be responsible for forming GG mismatches, the pattern of H bonds and stability may be examined. The numbering in this mismatch indicates the sites of prototropic tautomerization. The relative energy level of G tautomers is shown in Figure 5, some of the tautomers are found at close energy levels. In such situation the tautomers located at narrow energy levels may

form either GG mismatches or undergo tautomerization to another form.

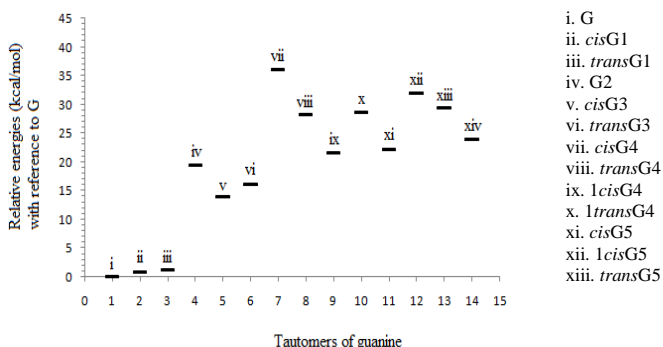


Figure 5: Variation of energies (6-31++G(d,p)) (kcal/mol) of G tautomers with respect to G. {Here, G→ amino guanine, $\Delta_1(i \rightarrow ii) = 0.729$ kcal/mol, $\Delta_2(i \rightarrow iii) = 1.257$ kcal/mol, $\Delta_3(i \rightarrow iv) = 19.459$ kcal/mol, $\Delta_4(i \rightarrow v) = 13.894$ kcal/mol, $\Delta_5(i \rightarrow vi) = 15.998$ kcal/mol, $\Delta_6(i \rightarrow vii) = 36.133$ kcal/mol, $\Delta_7(i \rightarrow viii) = 28.242$ kcal/mol, $\Delta_8(i \rightarrow ix) = 21.629$ kcal/mol, $\Delta_9(i \rightarrow x) = 28.538$ kcal/mol, $\Delta_{10}(i \rightarrow xi) = 22.242$ kcal/mol, $\Delta_{11}(i \rightarrow xii) = 31.961$ kcal/mol, $\Delta_{12}(i \rightarrow xiii) = 29.411$ kcal/mol, and $\Delta_{13}(i \rightarrow xiv) = 23.848$ kcal/mol}

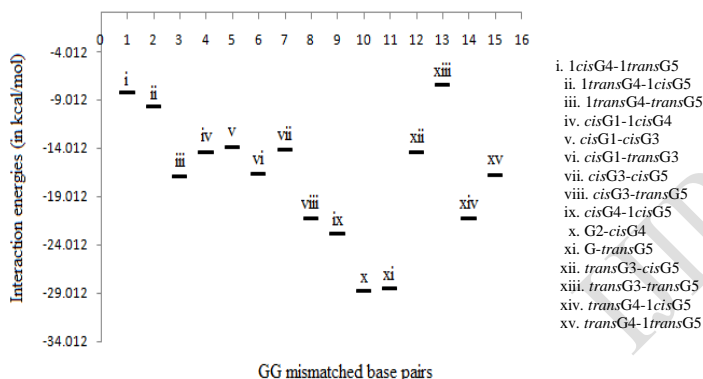
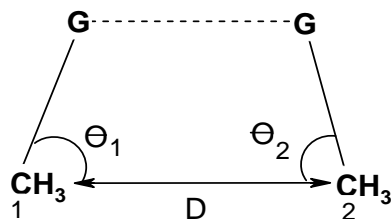


Figure 6: Comparison of interaction energies (6-31++G(d,p)) of metastable GG mismatches



Here, $CH_3 \rightarrow$ represents sugar backbone
 $D \rightarrow$ distance between methyl groups
 $\Theta_1 \rightarrow$ angle of inclination of CH_3 (1)
 $\Theta_2 \rightarrow$ angle of inclination of CH_3 (2)

Figure 7: The methyl-methyl distance and angles of inclination

Metastable GG Mismatches	Interaction energies (kcal/mol)		BSSE values (kcal/mol)
	B3LYP/6-31+G(d,p)		
1cisG4-1transG5 (i)	-8.293		1.068
1transG4-1cisG5 (ii)	-9.766		1.171
1transG4-transG5 (iii)	-16.894		1.689
cisG1-1cisG4 (iv)	-14.368		0.773
cisG1-cisG3 (v)	-13.894		0.833
cisG1-transG3 (vi)	-16.631		0.798
cisG3-cisG5 (vii)	-14.170		1.032
cisG3-transG5 (viii)	-21.251		1.062
cisG4-1cisG5 (ix)	-22.875		1.002
G2-cisG4 (x)	-28.767		1.619
G-transG5 (xi)	-28.518		1.165
transG3-cisG5 (xii)	-14.329		0.798
transG3-transG5 (xiii)	-7.381		0.687
transG4-1cisG5 (xiv)	-21.346		1.096
transG4-1transG5 (xv)	-16.790		0.781

Table 1: Computed interaction energies and BSSE values of GG mismatches with B3LYP/6-31+G(d,p) calculations

Metastable GG Mismatches	Interaction energies (kcal/mol)		BSSE energies (kcal/mol)
	B3LYP/6-31++G(d,p)		
1cisG4-1transG5 (i)	-8.230		1.002
1transG4-1cisG5 (ii)	-9.712		1.130
1transG4-transG5 (iii)	-16.954		1.767
cisG1-1cisG4 (iv)	-14.391		0.792
cisG1-cisG3 (v)	-13.954		1.122
cisG1-transG3 (vi)	-16.667		0.885
cisG3-cisG5 (vii)	-14.224		1.052
cisG3-transG5 (viii)	-21.293		1.094
cisG4-1cisG5 (ix)	-22.903		1.030
G2-cisG4 (x)	-28.784		1.686
G-transG5 (xi)	-28.530		1.223
transG3-cisG5 (xii)	-14.408		1.004
transG3-transG5 (xiii)	-7.408		0.714
transG4-1cisG5 (xiv)	-21.326		1.051
transG4-1transG5(xv)	-16.797		1.021

Table 2: Computed Interaction energies and BSSE energies of GG mismatches with B3LYP/6-31++G(d,p) calculation

Metastable GG Mismatches	Interaction energies (kcal/mol)	BSSE values (kcal/mol)
1cisG4-1transG5 (i)	-14.414	4.447
1transG4-1cisG5 (ii)	-15.574	4.157
1transG4-transG5 (iii)	-24.328	6.321
cisG1-1cisG4 (iv)	-18.183	3.999
cisG1-cisG3 (v)	-19.513	4.898
cisG1-transG3 (vi)	-19.684	4.410
cisG3-cisG5 (vii)	-18.468	4.892
cisG3-transG5 (viii)	-24.466	4.557
cisG4-1cisG5 (ix)	-26.932	3.741
G2-cisG4 (x)	-33.859	6.298
G-transG5 (xi)	-29.975	5.109
transG3-cisG5 (xii)	-17.779	4.217
transG3-transG5 (xiii)	-10.151	2.616
transG4-1cisG5 (xiv)	-25.441	3.996
transG4-1transG5 (xv)	-21.758	4.034

Table 3: Computed interaction energies and BSSE values of GG mismatches with MP2/6-31+G(d,p) calculations

Metastable GG Mismatches	Interaction energies in kcal/mol HF/6-31+G(d,p)
1cisG4-1transG5	-5.490
1transG4-1cisG5	-9.177
1transG4-transG5	-12.750
cisG1-1cisG4	-9.914
cisG1-cisG3	-10.054
cisG1-transG3	-11.683
cisG3-cisG5	-10.470
cisG3-transG5	-17.160
cisG4-1cisG5	-21.984
G2-cisG4	-23.744
G-transG5	-23.408
transG3-cisG5	-10.000
transG3-transG5	-5.029
transG4-1cisG5	-19.520
transG4-1transG5	-13.568

Table 4: Computed interaction energies of metastable GG mismatches with HF/6-31+G(d,p)

Metastable GG mismatches	Energies (kcal/mol)	Δ ZPE (kcal/mol)
--------------------------	---------------------	-------------------------

1cisG4-1transG5	-6.354 ^a , 2.751 ^b	-7.422
1transG4-1cisG5	-8.665 ^a , 2.641 ^b	-8.742
1transG4-transG5	-15.529 ^a , -3.618 ^b	-15.732
cisG1-1cisG4	-13.006 ^a , -0.204 ^b	-13.009
cisG1-cisG3	-11.742 ^a , -0.272 ^b	-12.141
cisG1-transG3	-15.386 ^a , -2.293 ^b	-15.327
cisG3-cisG5	-13.055 ^a , -1.444 ^b	-13.326
cisG3-transG5	-19.943 ^a , -8.537 ^b	-20.242
cisG4-1cisG5	-22.059 ^a , -7.002 ^b	-21.000
G2-cisG4	-27.721 ^a , -12.750 ^b	-26.943
G-transG5	-27.614 ^a , -16.090 ^b	-27.788
transG3-cisG5	-13.200 ^a , -2.150 ^b	-13.574
transG3-transG5	-7.293 ^a , 5.742 ^b	-6.872
transG4-1cisG5	-20.240 ^a , -6.856 ^b	-19.844
transG4-1transG5	-15.216 ^a , -4.254 ^b	-15.493

a → change of enthalpy (ΔH), b → change of free energy (ΔG)
Table 5: Computed ΔH , ΔG and ΔZPE of metastable GG mismatches with B3LYP/6-31+G(d,p) calculations

GG mismatches	H-bond distance (Å)	Planarity
1cisG4-1transG5 (i)	H _u →1.973 H _l →2.065	Twisted(15.71°)
1transG4-1cisG5 (ii)	H _u →2.139 H _l →2.320	Twisted(85.47°)
1transG4-transG5 (iii)	H _u →2.337* H _l →2.440*	Bent(137.53°)
cisG1-1cisG4 (iv)	H _u →1.942 H _m →1.994 H _l →1.896	Planar
cisG1-cisG3 (v)	H _u →1.672 H _l →1.939	Twisted(25.32°)
cisG1-transG3 (vi)	H _u →1.704 H _m →1.920 H _l →2.004	Planar
cisG3-cisG5 (vii)	H _u →1.637 H _l →1.919	Twisted(28.53°)
cisG3-transG5 (viii)	H _u →1.596 H _m →1.927 H _l →2.147	Planar
cisG4-1cisG5 (ix)	H _u →1.860* H _l →1.965*	Planar
G2-cisG4 (x)	H _u →1.714 H _l →1.916	Bent(94.92°)
G-transG5 (xi)	H _u →1.523 H _m →1.872 H _l →1.940	Planar
transG3-cisG5 (xii)	H _u →1.662 H _m →1.943 H _l →2.203	Planar

<i>transG3-transG5</i> (xiii)	$H_u \rightarrow 1.895^*$	Planar
<i>transG4-1cisG5</i> (xiv)	$H_u \rightarrow 1.872^*$ $H_l \rightarrow 1.866^*$	Planar
<i>transG4-1transG5</i> (xv)	$H_u \rightarrow 1.880$ $H_m \rightarrow 2.007$ $H_l \rightarrow 2.036$	Planar

The values inside the parenthesis () are torsional angle '*' indicates the skipped H-bond

Table 6: Computed H-bond distances and planarity in metastable GG mismatches (6-31++G(d,p)).

GG Mismatch	θ_1	θ_2	D(Å)
<i>1cisG4-1transG5</i> (i)	40.90°	42.65°	13.147
<i>1transG4-1cisG5</i> (ii)	47.51°	40.47°	13.058
<i>1transG4-transG5</i> (iii)	58.52°	32.29°	11.528
<i>cisG1-1cisG4</i> (iv)	43.93°	42.21°	13.163
<i>cisG1-cisG3</i> (v)	42.03°	42.03°	12.967
<i>cisG1-transG3</i> (vi)	41.51°	40.32°	13.175
<i>cisG3-cisG5</i> (vii)	41.04°	40.20°	13.060
<i>cisG3-transG5</i> (viii)	38.44°	39.86°	13.237
<i>cisG4-1cisG5</i> (ix)	32.31°	49.04°	13.418
<i>G2-cisG4</i> (x)	47.39°	50.34°	12.216
<i>G-transG5</i> (xi)	40.51°	40.25°	13.107
<i>transG3-cisG5</i> (xii)	38.76°	39.08°	13.294
<i>transG3-transG5</i> (xiii)	58.81°	81.34°	12.556
<i>transG4-1cisG5</i> (xiv)	32.63°	50.81°	13.381
<i>transG4-1transG5</i> (xv)	42.35°	40.05°	13.264

Here, θ_1 and θ_2 are angle of inclination and 'D' is the distance between the two sugar rings.

Table 7: Distances between two methyl groups representing sugar and angles of inclination of different GG mismatches (6-31++G(d,p)).

A. HYDROGEN BOND TYPES IN METASTABLE GG PAIRS

- ✓ In *1cisG4-1transG5* combination, two H-bonds types are involved in pairing. There are imine-imine type of H bond on tautomerization of exocyclic amine groups and >N-H....N< type of hydrogen bonding between N of purine rings (Figure 4(i)).
- ✓ Another metastable GG combination is *1transG4-1cisG5*, which is stabilized by two types of H-bonds (Figure 4(ii)). These types of H bonds are similar to that of *1cisG4-1transG5* but the orientations of H bonds are different. The imine-imine type and >N-H....N< types are present.
- ✓ The *1transG4-transG5* is stabilized by -N-H...imine group (between ring nitrogen and exocyclic imine group). The methyl group representing sugar in *transG5* is found inverted after pairing in the optimum structure (Figure 4(iii)). It may be due to weak H bonding capacity that is not sufficient to maintain the methyl group at the original configuration.

- ✓ The hydrogen bonding pattern in *cisG1-1cisG4* are enol-enol type, between >N-H...N< ring nitrogens and amino-imine type (Figure 4(iv)). Although like other mismatches, type of >N-H....N< H-bond is common, the H bond length is different from other mismatches (Table 6). This may be due to the effect of other H bonds present in this mismatch.
- ✓ In *cisG1-cisG3*, the hydrogen bonds are keto-enol and >N-H...N< types (between ring nitrogens). The hydrogen bond lengths are shown in Table 6 (Figure 4(v)).
- ✓ The *cisG1-transG3* is stabilized by three hydrogen bonds. The keto-enol type, >N-H....N< type and amine-imine type of bonds are found (Figure 4(vi)). The H bonding orientations are different from other mismatches (Table 6).
- ✓ *cisG3-cisG5* is stabilized by two types of H bonds, keto-enol type and >N-H...N< type (Figure 3.4(vii)). Both the hydrogen bond lengths are found comparatively longer than those in other mismatches (Table 6).
- ✓ Three types of hydrogen bonds are found in *cisG3-transG5*. In addition to keto-enol type and >N-H....N< type bonding, another type imine-imine type of H bonding is found (Figure 4(viii)). The H bond lengths and planarity of H bonds are given in Table 6.
- ✓ *cisG4-1cisG5* is stabilized by entirely different types of H bonds (Figure 4(ix)). The enol-N(ring) and ring N-imino type of H bonds are found. From the H bond lengths and orientation of bonds, these H bonds may not be strong (Table 6).
- ✓ Although only two types of H bonds are present in *G2-cisG4*, this is the most favorable combination. The keto-enol and >N-H....N< types are present (Figure 4(x)). The H bond lengths are comparatively small and it appears that the orientation of H bonds may be considered for maintaining stable combination (Table 6).
- ✓ *G-transG5* is the second most stable combination. In addition to keto-enol, >N-H...N< type of bonding, another amino-imine type of bonding is present (Figure 4(xi)). The H bond lengths as well as the orientations of H bonds are shown in Table 6. So, it may not be necessary to have three H bonding for favorable combination of GG mismatches. The H bond orientation may be another factor for effective pairing.
- ✓ There are three types of H bonds in *transG3-cisG5*, the common keto-enol, >N-H....N< and imine-imine types are found (Figure 4(xii)). The H bond lengths and orientations of bonding are given in Table 6.
- ✓ Only one type of H bond is found in *transG3-transG5* (Figure 4(xiii)). The hydrogen bond between ring N and imine is found. This pairing may be less favorable compared to other mismatches. Moreover the hydrogen bond length is less than 2Å and non-planar (Table 6).
- ✓ In *transG4-1cisG5* two types of H bonds are present. One is enol-N(ring) and the other one is ring N-imine (Figure 4(xiv)). The H-bond lengths and angles are given in Table 6.
- ✓ Three types of H bonds are found in *transG4-1transG5*. The enol-enol type, >N-H...N< (between ring N) and imine-imine type of bonds are found (Figure 4(xv)).

Likewise H bond distances and orientation of these bonds are given in Table 3.6.

The distances (D) between the two methyl groups representing sugar are also measured. These distances are very different for all these metastable mismatches (Figure 7, Table 7). Moreover, the angles of inclination, θ_1 and θ_2 are also measured. It is possible to understand how such mispairing result deformation in helix. The values of D are between 12-13 Å and the values of θ_1 and θ_2 are small and unequal (32.31° and 49.04°) for *cisG4-1cisG5* (ix) compared to other mismatches. The D value is 13.418 Å. However for the most favorable pair, *G2-cisG4* (x) the θ_1 and θ_2 values are 47.39° and 50.34° , and D value is 12.216 Å. The variation of these values may be due to H bonding capacity of the bonds towards methyl groups compared to the other bonds present opposite to methyl groups. Subsequently the angle of inclinations are also changed (Table 7).

The types of H-bonds present in most GG mismatches are (a) $>N-H\dots N<$ (between ring N) (b) $-O-H\dots O=C-$ (keto-enol) (c) $-O-H\dots O-C-$ (enol-enol) (d) $-N-H\dots N=C-$ (amine-imine) (e) $-O-H\dots N<$ (enol-ring N) (f) $>N-H\dots N=C-$ (ring N-imine) (g) $-C=N\dots H-N=C-$ (imine-imine), and (h) $-O-H\dots N=C-$ (enol-imine).

As we can see in all structures, the H bond types $>N\dots H-N<$ and keto-enol are present in many metastable GG pairs. These bonds may contribute efficient stabilization. The H-bond type $-N-H\dots N=C-$ (amine-imine), $>N-H\dots N=C-$ (ring N-imine), $-O-H\dots N<$ (enol-ring N) and $>N-H\dots N=C-$ (ring N-imine) are found only in some pairs (Table 6). The stability of these metastable mismatches may be analysed from the interaction energies and thermodynamic parameters with respect to these different types of H bonds.

B. STABILITY OF METASTABLE GG MISMATCHES

The computed interaction energies with B3LYP/6-31+G(d,p) and B3LYP/6-31++G(d,p) are shown in Table, the values are reasonably a large negative for some metastable GG pairs (Tables 1 and 2). The H-bond lengths in these structure are quite short ($<2\text{Å}$) and maintain a planar structure. The H bonding capacity of the types of H-bonds present in these stable pairs *G2-cisG4*, *G-transG5* and *transG3-cisG5* may be responsible for favorable pairing (Table 6). On the other hand, *transG3-transG5* is comparatively less stable combination and type of H bond present in this pair is different from those of stable pairs. The interaction energy of this metastable mismatch is -7.408 kcal/mol, so it may form once the G tautomers are generated. The presence of only one H-bond may be the reason for less stability of this combination. The *transG4-1cisG5* (xiv) and *transG4-1transG5* (xv) are less stable combination inspite of the presence of similar types of H-bonds. So, it appears that H-bond types (a) and (b) contribute to better stability of these metastable structures. It is not feasible to estimate the strength of these bonds separately, but it is possible to guess H bonding capacity indirectly from the H-bond lengths and interaction energies (Figures 4(i-xv)), Table 6). The computed single point MP2/6-31+G(d,p) on the B3LYP/6-31+G(d,p) optimized geometry also shows similar trend of stability of these mismatches.

We have also examined the planarity and torsional angles of H bonds that also reflect the extent of distortion of sugar backbones due to tautomer pairing (Table 6). From these values the change of DNA conformation due to the presence of GG mismatches may be understood indirectly. The values may be related to the H-bonding capability, where effective H-bond is expected if H bond distance is short. Also in turn elongation or squeezing of sugar backbone may take place depending on the presence of stronger H-bond towards the sugar side or on the other side of sugar backbone. Hence, these metastable mismatches may initially form once G tautomers are generated in DNA.

Based on the hydrogen bonding properties the results of B3LYP with basis sets 6-31+G(d,p) and 6-31++G(d,p) of metastable GG tautomers are energetically stable and the interaction energies are given in (Tables 1-2) and also BSSE values are also shown separately. Hence, instantaneous pairing of G tautomers is possible. The contribution of three types of H bonding to the stability of metastable GG mismatches is suggested. Table 3 shows the MP2/6-31+G(d,p) results computed on the optimized geometries of B3LYP/6-31+G(d,p). The variation of interaction energies obtained from B3LYP and MP2 with basis set 6-31+G(d,p) is similar and the thermodynamic parameters given in table 5 also provide information on the stable GG combination. So the H-bonding capacity of different types of H-bonds in various metastable GG pairs is very important to form energetically favorable pairs. Similarly, the trend in the interaction energies (ΔE) with respect to the pattern of H-bonds present in GG pairs may be analysed and the presence of H bond types $-O\dots H-O-$ and $>N\dots H-N<$ in some of these structures produces better stabilization (Figure 4, Table 6). As observed in Tables 1-4, the interaction energies for *G2-cisG4* (x) is comparatively large, the presence of $=O\dots H-O-$ and $>N\dots H-N<$ types of bonding is found in this pair. The interaction energy for this pair computed with B3LYP/6-31++G(d,p) for the most stable structure is -28.784 kcal/mol.

In all these metastable GG combinations, tautomer selectivity in pairing may be related to the hydrogen bonding capacity of H bonds. The energy level of G tautomers that certain tautomers are found at close energy level but it is not necessary that pairing of these G tautomers lead to favorable metastable pairs (Figure 5). It is not necessary that those tautomers located at close energy levels prefer to pair up to form stable metastable mismatches. The stability of metastable GG combination can be visualized from Figure 6. The difference in interaction energies is not so large for some metastable GG pairs. The structure of *transG4-1cisG5* (xiv) combination is found somewhat very close to crystal structure. But stacking interaction among purine rings might contribute to the displacement of H bonding pattern in crystal structures (Figures 1(i-ii)). As we know that many other factors may influence the crystal structure such as solution pH and the effect of other ions. These metastable GG mismatches may undergo transformation to other structures through proton transfer mechanism. However, it is possible to extract certain information from these metastable GG mismatches to explain the existence of GG mismatches.

IV. CONCLUSION

The DFT and MP2 levels of studies performed on the metastable GG tautomer combination clearly indicate the formation of metastable GG pairs. The results of both DFT and MP2 calculations equally predict the stable pairs from G tautomers. Several types of H bonds are likely to contribute to these stable structures. The interaction energy of most favorable metastable GG combination obtained from B3LYP/6-31++G(d,p) is -28.784 kcal/mol, and some of the pairs are found at very close energy levels. The presence of different types of H bonds contributes to better stabilization of mismatches. The computed thermodynamic properties equally predict the formation of GG tautomer combinations. Hence, from this viewpoint the instantaneous G tautomer pairing might be responsible for the occurrence of GG mismatches in DNA. The structure and H bonding in *trans*G4-1*cis*G5 is somewhat similar to crystal structure, but the formation of tautomers cannot be exactly known from crystal structure.

REFERENCES

- [1] J. Li, H. He, X. Peng, M. Huang, X. Zhang, S. Wang, *Analytical Sciences*. 31 (2015) 663-667.
- [2] J.A.H. Cognet, J. Gabarro-Arpa, M. Le Bret, G.A. van der Marell, J.H. van Boom, G.V. Fazakerley, *Nucleic Acids Res.* 19 (1991) 6771-6779.
- [3] A.N. Lane, B. Peck, *Eur. J. Biochem.* 230 (1995) 1073-1087.
- [4] B. Lippert, D. Gupta, *Dalton Trans.* 24 (2009) 4619-4634. DOI: 10.1039/b823087k
- [5] G. Natrajan, M.H. Lamers, J.H. Enzlin, H.H.K. Winterwerp, A. Perrakis, T.K. Sixma, *Nucleic Acids Res.* 2003, 31: 4814 DOI: 10.2210/pdb1oh7/pdb NDB: PD0663
- [6] S.J. Johnson, L.S. Beese, *Cell (Cambridge, Mass.)* 2004, 116: 803-816.
- [7] J.V. Skelly, K.J. Edwards, T.C. Jenkins, S. Neidle, *Proc. Natl. Acad. Sci. USA* 1993, 90: 804-808. DOI: 10.2210/pdb1d80/pdb NDB: BDL046
- [8] V.I. Danilov, V.M. Anisimov, N. Kurita, D. Hovorun, *Chem. Phys. Lett.* 412 (2005) 285-293.
- [9] A. Perez, M.E. Tuckerman, H.P. Hjalmarson, O.A. von Lilienfeld, *J. Am. Chem. Soc.* 132 (2010) 11510-11515.
- [10] I.O. Navas, J.M. Seminario, *J. Mol. Model.* DOI: 10.1007/s00894-011-1028-1.
- [11] S.T. Madariaga, J.G. Contreras, *J. Chil. Chem. Soc.* 55, N° 1 (2010)
- [12] A.J.A. Aquino, D. Nachtigallova, P. Hobza, D.G. Truhlar, C. Hattig, H. Lischka, *J. Comput. Chem.* 32 (2011) 1217-1227.
- [13] J.P. Ceron-Carrasco, J. Zuniga, A. Requena, E.A. Perpete, C. Michaux, D. Jacquemin, *Phys. Chem. Chem. Phys.* 13 (2011) 14584-14589.
- [14] S. Urashima, H. Asami, M. Ohba, H. Saigusa, *J. Phys. Chem. A* 114 (2010) 11231-11237.
- [15] B. Lippert, *J. Chem. Soc., Dalton Trans.* 21 (1997) 3971-3976.
- [16] D. Nachtigallova, T. Zeleny, M. Ruckebauer, T. Muller, M. Barbatti, P. Hobza, H. Lischka, *J. Am. Chem. Soc.* 132 (2010) 8261-8263.
- [17] M. Suzuki, K. Kino, M. Morikawa, T. Kobayashi, H. Miyazawa, *Molecules*. 19 (2014) 11030-11044. doi:10.3390/molecules190811030
- [18] S.C.N. Hsu, T.P. Wang, C.L. Kao, H.F. Chen, P.Y. Yang, H.Y. Chen, *J. Phys. Chem. B* 117 (2013) 2096-2105.
- [19] J. Spöner, M. Sabat, L. Gorb, J. Leszczynski, B. Lippert, P. Hobza, *J. Phys. Chem. B* 104 (2000) 7535-7544.
- [20] N. Russo, M. Toscano, A. Grand, F. Jolibois, *J. Comput. Chem.* 19 (1998) 989-1000.
- [21] A. Karton, R.J. O'Reilly, L. Radom, Assessment of Theoretical Procedures for Calculating Barrier Heights for a Diverse Set of Water-Catalyzed Proton-Transfer Reactions, *J. Phys. Chem. A* 116 (2012) 4211-4221.
- [22] M. Rueda, F.J. Luque, J.M. Lopez, M. Orozco, *J. Phys. Chem. A* 105 (2001) 6575-6580.
- [23] W. Zierkiewicz, D. Michalska, P. Hobza, *Phys. Chem. Chem. Phys.* 12 (2010) 2888-2894.
- [24] J. Rezac, P. Hobza, S.A. Harris, *Biophys. J.* 98 (2010) 101-110.
- [25] A. Tikhomirova, I.V. Beletskaya, T.V. Chalikian, *Biochemistry*. 45 (2006) 10563-10571.
- [26] M.J. Frisch, G.W. Trucks, H.B. Schlegel, G.E. Scuseria, M.A. Robb, J.R. Cheeseman, J.A. Jr Montgomery, T. Vreven, K.N. Kudin, J.C. Burant, J.M. Millam, S.S. Iyengar, J. Tomasi, V. Barone, B. Mennucci, M. Cossi, G. Scalmani, N. Rega, G.A. Petersson, H. Nakatsuji, M. Hada, M. Ehara, K. Toyota, R. Fukuda, J. Hasegawa, M. Ishida, T. Nakajima, Y. Honda, O. Kitao, H. Nakai, M. Klene, X. Li, J.E. Knox, H.P. Hratchian, J.B. Cross, V. Bakken, C. Adamo, J. Jaramillo, R. Gomperts, R.E. Stratmann, O. Yazyev, A.J. Austin, R. Cammi, C. Pomelli, J.W. Ochterski, P.Y. Ayala, K. Morokuma, G.A. Voth, P. Salvador, J.J. Dannenberg, V.G. Zakrzewski, S. Dapprich, A.D. Daniels, M.C. Strain, O. Farkas, D.K. Malick, A.D. Rabuck, K. Raghavachari, J.B. Foresman, J.V. Ortiz, Q. Cui, A.G. Baboul, S. Clifford, J. Cioslowski, B.B. Stefanov, G. Liu, A. Liashenko, P. Piskorz, I. Komaromi, R.L. Martin, D.J. Fox, T. Keith, M.A. Al-Laham, C.Y. Peng, A. Nanayakkara, M. Challacombe, P.M.W. Gill, B. Johnson, W. Chen, M.W. Wong, C. Gonzalez, J.A. Pople, (2004) Gaussian 03, Revision C.02. Gaussian Inc, Wallingford CT.